The effect of Stachys floridana *Shuttlew.ex Benth extract as an additive on the chemical properties of chitosan biodegradable film*

QINGXUAN ZHAO, SHUN LIU, JIE LI, HAITANG LIU, SHENG LIU, QIAN WANG, YING LI, AND HUI WANG

ABSTRACT: The purpose of this study is to explore chitosan with *Stachys floridana* Shuttlew. ex Benth (SFSB) extract as an additive to prepare an active film. The effects of the SFSB extract on the physical, antioxidant, and bacteriostatic properties of chitosan biodegradable films were studied. The results showed that the addition of SFSB extract significantly improved the antioxidant and antibacterial properties of the film, and its biodegradation rate increased rapidly. Compared to the control film, the water solubility was lower at 19.40%, the expansion degree was higher at 288.90%, the water vapor permeability (WVP) was 0.364 g·mm/(m^2·d·kPa), the surface hydrophobicity increased, and the mechanical strength was also improved. The contact angle increased to 89.3°. In addition, as the amount of SFSB increased, the thermal stability of chitosan-*Stachys floridana* Shuttlew. ex Benth (CS-SFSB) films also increased significantly, and their ultraviolet (UV) blocking ability was gradually enhanced. The results indicate that CS-SFSB has potential as a food packaging material.

Application: This work is conducive to the development of CS-based films and contributes to the development of new biodegradable food packaging films.

In recent years, the excessive use of oil-based plastic products has not only caused serious pollution to the environment, it has also posed a huge hidden danger to ecosystem balance and human health. As a result, a number of researchers are actively exploring new packaging materials. Plant-derived extracts or powders are added to packaging films, especially edible films made from fruit and vegetable puree, pulp, juice, or extract, and have been attracting more and more attention due to their characteristics of easy processing, edible applicability, and easy degradation [1-3]. Different plant extracts have obvious differences in composition that endow films with special functionality. When the extract is added to the biofilm, it interacts with the film matrix, thus improving the structural physical properties (hydrophobicity, tensile strength, thermal stability) and biological properties (anti-oxidation, antibacterial) [4]. Therefore, it is important to explore the application of biological active materials in the development of biodegradable films.

Chitosan is a common component in the shell of arthropods, fungi, and algae cell membranes and high plant cell walls. Chitosan is the second largest natural polymer, and its free amino molecules make it the only known alkaline natural polysaccharide to date [5]. Because of its rich unsaturated groups, chitosan has remarkable biological characteristics that are embodied in biodegradability, biocompatibility, and anti-oxidation, which bestow it with common use as a film matrix. Different plant extracts, such as grape [6], pine needle [7], allium tuberosum [8], green tea [9], aloe vera [10], and mango leaf [11], can be used to improve the antioxidant properties and bacteriostatic properties of chitosan (CS) film.

Stachys floridana Shuttlew. ex Benth (SFSB), belonging to the genus labia, is a perennial herb, and is found mainly in Luoyang, Henan province, China. Its roots are rich in nutrients, such as protein, carbohydrates, fats, amino acids, and polyphenols. It not only has good edible value, but also has high medicinal value. According to scientific research, the extract of silver food has a variety of biological activities, such as immune regulation [12], intestinal probiotics [13], hypoglycemia [14], bacteriostasis [15], anti-inflammation [16], and antitumor activity [17,18]. Previous studies have found that its extracts also have excellent antioxidant properties, but in reality, SFSB is used only as a vegetable, the duration of preservation is short, and its biological value cannot be effectively developed. So far, the use of SFSB extract as a potential natural additive to improve the antioxidant activity of biomaterials has not been studied.

Therefore, the purpose of this study is to combine chitosan with SFSB extract to prepare an environmentally friendly active film. Through the systematic analysis and detection of the physical properties, mechanical properties, antioxidant activity, bacteriostatic properties, and biodegradability of the composite film, the results demonstrat-

ed excellent mechanical properties and thermal stability. Additionally, the composite film also exhibited outstanding performance in terms of anti-oxidation and antibacterial properties. Consequently, the composite film has the potential to be applied to food packaging bags.

In summary, this paper introduces a new plant extract (SFSB) into the research field of CS films and comprehensively evaluates its impact on the properties of CS films, especially the remarkable improvement in biodegradability, through systematic experiments and analysis. This provides new ideas and contributions to the research in this field.

MATERIALS AND METHODS

Materials and reagents

The following materials and reagents were used: chitosan (deacetylation degree ≥95%) from Shanghai Aladdin Biochemical Technology Co. Ltd.; phenol,bovine serum protein from Beijing Solaibao Technology Co. Ltd.; Coomassie Brilliant Blue (G-250) from Fuchen (Tianjin) Chemical Reagent Co.; forlinphenol reagent from Shanghai Yihui Biotechnology Co. Ltd.; 1,1-diphenyl-2-picrylhydrazyl from Tokyo Chemical Industry Co. Ltd.; 2, 2'-azino-bis(3-ethylbenzothiazoline-6-sulfonic acid from Shanghai Maclin Biochemical Technology Co. Ltd.; galacturonic acid from Shanghai Ruiyong Biotechnology Co. Ltd.; and gallic acid, acetic acid, ethanol, glycerin, and potassium bromide from Sinopharm Pharmaceutical Group Co. Ltd.

Methodology

Preparation of SFSB extract

Fresh silver sliver vegetables were purchased from the farmer's market in Yanshi, Luoyang City. They were rinsed with deionized water, vacuum-dried at 60°C, and then ground into powder by a high-speed universal mill (40–200 mesh) and screened through 80 mesh. The powder was mixed with water at a 1:30 liquid-to-solid ratio, followed by ultrasonic extraction (180 W, 53 kHz) for 30 min. The residue was removed by filtration, and the extraction solution was concentrated to one-fifth of the original volume at 50°C. Anhydrous ethanol was added to make the ethanol concentration reach 80%, and the solution was placed in the refrigerator at 4°C overnight. Finally, the precipitation and supernatant were separated, and the precipitation was frozen and freeze-dried in a cold dryer to obtain SFSB. Freeze-dried samples were stored at -20°C.

Composition analysis of extract

Determination of total carbohydrate: According to the research method of Lin et al. [19], the total carbohydrate content of the sample was determined. Using glucose as the standard, standard solutions with different concentration gradients were added to the test tubes, and distilled water was added to make the total volume up to 2 mL. Then, 1 mL of 5% phenol solution was added to the mixture, followed by 5.0 mL of concentrated sulfuric acid (98%). The mixture was thoroughly mixed and left to stand for 20 min. Distilled water was used as the blank, replacing the standard solution, and the absorbance was measured at 490 nm using an ultraviolet (UV) spectrophotometer. The absorbance of the diluted sample solution was determined using the above-mentioned method, and its content was calculated.

Determination of total phenol content: A colorimetric method was used to determine polyphenols in samples, with slight modifications to the methods of Li et al. [20]. Using gallic acid as the standard, the standard solution was prepared to a concentration of 100 µg/mL, and standard sample dilutions with the same concentration gradient were also prepared. Then, 1.0 mL of the standard sample dilution was mixed with 1.0 mL of forlinphenol reagent (0.25 mol/L), allowed to stand for 3 min, and then 2.0 mL of 15% sodium carbonate (Na_2CO_3) solution was added. The mixture was well mixed and allowed to stand for 30 min. Using 15% Na_2CO_3 solution as the blank control, the absorbance was determined by a UV spectrophotometer at 760 nm. The absorbance of 1.0 mL of the diluted sample solution was determined according to the above steps, and the total phenol content of the sample solution was calculated.

Determination of protein content: The Coomassie Brilliant Blue method [21] was used to determine the protein content in the extract. The absorbance of bovine serum protein was measured at 595 nm using a UV spectrophotometer to determine the protein content in the extract.

Determination of uronic acid content: The modified carbazole-sulfuric acid method was used to determine the content of uronic acid in the extract. Taking galacturonic acid as the standard, it undergoes a condensation reaction with carbazole reagent in sulfuric acid and is then quantified by a colorimetric spectrophotometer at 530 nm. Based on the measurement results, the amount of chitosan used for film preparation is 2.0% w/v.

Film preparation

The preparation of CS film was based on the previous literature and improved according to the method described by Chen et al. [22] and Jiang et al. [23] et al. First, chitosan was mixed with 1.0% acetic acid solution, and stirred vigorously at 50°C (1000 rpm) for 2 h to prepare 2.0% w/v CS film-forming solution. Then, glycerin (30% d/w based on chitosan) was added into the CS film-forming solution as a plasticizer and further stirred for 30 min. Extracts (10%, 20%, 30%, 40% d/w) of the CS were added to CS film-forming solution in different proportions based on CS amount, which are hereafter referred to as SFSB-10, SFSB-20, SFSB-30, and SFSB-40, respectively. The effects of the different contents of chitosan on the film properties were studied. After mixing, the extracts were stirred at 800 rpm for 1 h at room temperature. The resulting mixed solution was degassed using ultrasound (200W) for 15 min to remove bubbles. Finally, the degassing solution was poured on PVC

petri dish with a diameter of 9 cm, and then the petri dish was placed in an oven at 50°C ± 0.2°C to dry for 24 h. After drying, the film was removed and placed in a room with a constant temperature and relative humidity (RH) of 25°C ± 0.2°C and 50% RH, respectively. The experiment was carried out for 48 h.

Physical properties of thin films

Thickness, moisture content, swelling degree, and water solubility

The thickness of the film was measured by a calibrated thickness meter (Lorentzen & Wettre; Kista, Sweden) that measured at 10 different positions of each film, and the values were expressed as an average. The moisture content (MC) of the film was calculated by the weight loss of the film sample after it was dried to a constant weight at 105°C [24]. The film sample, which had been dried to constant weight, was immersed in 30 mL of distilled water (25°C) for 24 h. Then, it was taken out and wiped dry with filter paper. The swelling degree (SD) of the film was measured by weighing it immediately [23]. The weighed film was baked in the oven at 105°C until it reached a constant weight, and the water soluble value (WSV) percentage was calculated [4].

Water contact angle

For measuring water contact angle (WCA), Stalder [25] et al.'s method was adopted to measure the surface hydrophobicity of each film with a contact angle tester. A drop of distilled water (2 mL) was dropped onto the surface of the sample. The angle (θ) formed by the intersection of the liquid-solid interface (the water droplets on the film surface) and the liquid-gas interface (the tangent line of the water droplets' boundary) was measured. Each sample was measured 10 times, and the average value was calculated.

Water vapor permeation analysis

Water vapor permeation (WVP) was measured using the weight reduction method, where the film was cut into a 7.40-cm-diameter circle, and the test cup containing 10 mL of distilled water was covered with the film sample. The sealing ring was placed, and the screw was tightened to seal it and prevent leakage. Then, the cups were placed into the test box (Model W-B-121F, Westang Technology; Mianyang, China) at conditions of 25°C ± 0.1°C and 75 ± 1% RH. Each test cup was weighed every 30 min. The weight difference of the test cup before and after 24 h was observed, and the water vapor transmission rate (WVTR) was measured using a humidity sensor. The WVP (g·mm/m²·d·KPa) was calculated using the following formula [9,10]:

$$WVP = \frac{WVTR \cdot X}{\Delta P} \quad (1)$$

where X is the film thickness (mm), and ΔP is the partial vapor pressure difference on both sides of the film (KPa).

Fourier transform infrared analysis

The dried potassium bromide (KBr), 150 mg, and the sample (1–2 mg) were mixed and fully ground. After pressing, the spectrum scanning was performed on the Nicolet iS5 Fourier transform infrared (FTIR) spectrometer (Thermo Fisher Scientific; Waltham, MA, USA) in the range of 400–4000 cm^{-1}. The FTIR spectrum of the film is obtained by switching the infrared spectrometer into attenuated total reflectance (ATR) mode, placing the film directly under the probe, and conducting full-band spectral scanning of the film.

Scanning electron microscope analysis

The surface morphology of the films was observed by scanning electron microscopy (SEM). The film was cut into a 1 cm × 1 cm square and placed on the metal post. After sputter coating with gold, the SEM image was taken.

Thermogravimetric analysis

The samples (2.0–10.0 mg) were placed in an aluminum pot in a thermogravimetric balance and then heated in a dry nitrogen atmosphere of 50 mL/min at a heating rate of 10°C/min and a temperature range of 40°C–400°C.

By setting the horizontal axis to represent temperature or time and the vertical axis to represent the mass percentage of the sample, two types of thermogravimetric analysis (TGA) curves can be plotted. A differential process is applied to the TGA curve with time as the horizontal axis and using the finite difference method to calculate the rate of mass change (dm/dT) or the rate of mass loss at each data point. The curve is then plotted with temperature on the horizontal axis and the rate of mass change (dm/dT) on the vertical axis. This curve is the derivative thermogravimetry (DTG) curve.

Color, whiteness, and opacity

The optical properties of the composite films were studied by measuring color, opacity, and whiteness. The color parameters of the films, including L* (luminosity), a* (red-green), and b* (yellow-blue), whiteness, and opacity, were determined using a calibrated instrument (Lorentzen & Wettre) that was calibrated with a standard whiteboard and a black tube.

Ultraviolet scanning spectroscopic analysis

The light transmittance of the film (4 cm × 4 cm) was scanned using a UV-visible spectrophotometer (UV-2700, Shimadzu, Japan) to determine the UV-Vis light blocking properties in the 200–800 nm range.

Mechnical strength

The tensile strength (TS) and elongation at break (EB) of the films were tested using a universal testing machine equipped with a 200 N load cell (Shanghai Lux Instruments Co. Ltd., China), according to the methods described in [26,27]. First, the film was cut into strips of specific dimen-

sions (80 mm × 10 mm). Then, the thickness of the cut film strips was measured using a thickness gauge. Subsequently, fixing the cut and measuring the film samples onto the clamping device of the equipment was performed. The mechanical properties were measured at a clearance of 40 mm and a velocity of 5 mm/s. Each sample was tested 10 times to ensure the accuracy and reliability of the data.

Antioxidant activity

DPPH free radical scavenging test

The methods of measuring DPPH (2,2-diphenyl-1-picrylhydrazyl) according to Silva et al. [27] and Li et al. [28] were slightly modified. In short, film samples of different weights were placed in a test tube containing 4 mL of 100 µmol/L DPPH ethanol solution. The test tube was then placed into an ultrasonic cleaner (220 V, 50 Hz), covered, and allowed to react at room temperature in the dark for 15 min. Subsequently, the absorbance of the reaction solution at 517 nm was measured using an ultraviolet spectrophotometer. The free radical scavenging rate inhibitory equation is as follows:

$$DPPH\ free\ radical\ scavenging\ rate\ (\%) = \frac{A0 - A1}{A0} * 100 \quad (2)$$

where *A0* and *A1* represent the absorbance of blank and reaction solution, respectively.

ABTS clearance rate

The 2,2'-Azino-bis(3-ethylbenzothiazoline-6-sulfonic acid) (ABTS) scavenging activity was determined according to the method described by Li et al. [28]. The ABTS diammonium salt reserve solution (7.4 mmol/L) and potassium persulfate ($K_2S_2O_8$) reserve solution (2.6 mmol/L) were mixed in a 1:1 (v/v) ratio and placed in a dark environment at room temperature for 12 h. Before use, the mixture was diluted 20–30 times with a phosphoric acid buffer solution of pH 7.4 until the absorbance at 734 nm reached 0.70 ± 0.02; at this point, the solution was considered the ABTS working fluid. Next, 4.0 mL of the ABTS working fluid was taken and a film sample of different quality was added. The solution was thoroughly mixed to ensure even distribution of the film. The working fluid without sample was used as the blank. The test tube was placed in the dark for 30 min to allow the reaction to occur, and then the absorbance was measured as follows:

$$ABTS\ clearance\ rate\ (\%) = \frac{A0 - Ai}{Ai} * 100 \quad (3)$$

where *Ai* and *A0* represent the absorbance value of ABTS solution with and without samples, respectively. All measurements were made three times.

Antibacterial property

We incorporated certain modifications into the disk diffusion method, as described by Genskowsky et al. [29] and Sun et al. [30], to assess the antibacterial capabilities of various CS films. *Escherichia coli* and *Staphylococcus aureus* were inoculated in the nutrient AGAR medium with 106 CFU/mL for each microbe and then evenly spread on the AGAR plate surface. A 7-mm-diameter filter paper was soaked in a different CS film solution and left at room temperature for 15 min to allow the film solution to spread before being placed on each plate. The diameter of the antibacterial zone (mm) was measured after 24 h incubation in the incubator.

Biodegradability

Biodegradation tests were conducted according to methods described by Medina Jaramillo et al. [31] and Piñeros-Hernandez [32], with some modifications. About 4 cm of soil was poured into a glass dish with a diameter of 20 cm and a depth of 5 cm. The soil was collected from under trees on the Tianjin University of Science and Technology campus. The samples (20 mm × 20 mm) were buried into 1–2 cm of soil. The soil was carefully dissected at different times (day 0, day 7, day 14), and the degradation process was monitored by visually examining the buried film. Samples were collected periodically and photographed.

Statistical analysis

All experiments involved at least three parallel experiments with data expressed as mean standard deviation. The statistical significance of the intergroup error was analyzed by one-way ANOVA, with $p < 0.05$ considered as statistically significant.

RESULTS AND DISCUSSION

Composition analysis of SFSB

The SFSB composition obtained by approximate analysis is shown in the **Table I**. The SFSB is mainly composed of carbohydrates, proteins, uronic acid, and polyphenols. Although there is no authoritative literature that specifies a standard range for the content of various components in plant extracts, based on common sense and experience, the content of various components in SFSB is in line with expectations.

Component	Composition, %
Carbohydrates	77.82
Glucuronic acid	6.31
Total proteins	1.03
Total phenol	0.53
Moisture	7.97

I. Approximate component analysis of* Stachys floridana *Shuttlew. ex Benth (SFSB).

Films	Thickness, mm	MC, %	SD, %	WS, %	WVP, gmm/(m²d.Kp)	WCA
CS	0.0544 ± 0.0002[a]	21.89 ± 0.14[a]	488.69 ± 0.14[a]	29.07 ± 0.14[a]	0.456 ± 0.007[a]	75.6 ± 0.1[a]
SFSB-10	0.0597 ± 0.0001[b]	20.19 ± 0.13[b]	340.83 ± 0.05[b]	25.28 ± 0.04[a]	0.432 ± 0.011[b]	77.9 ± 0.2[b]
SFSB-20	0.0638 ± 0.0002[c]	19.44 ± 0.07[c]	338.45 ± 0.17[d]	23.40 ± 0.08[b]	0.384 ± 0.014[c]	83.6 ± 0.1[c]
SFSB-30	0.0656 ± 0.0003[d]	15.51 ± 0.09[b]	307.23 ± 0.10[c]	20.17 ± 0.19[c]	0.376 ± 0.006[b]	87.2 ± 0.2[c]
SFSB-40	0.0704 ± 0.0002[c]	15.24 ± 0.05[d]	288.90 ± 0.06[b]	19.40 ± 0.21[d]	0.364 ± 0.012[c]	89.3 ± 0.3[d]

CS: chitosan; SFSB: *Stachys floridana* Shuttlew. ex Benth; MC: moisture content; SD: swelling degree; WS: water solubility; WVP: water vapor permeability; WCA: water contact angle.
Values were expressed as mean ± standard deviation, and each experiment was repeated at least three times. Values with different superscript letters (a-d) indicated significant differences by Tukey's test ($p < 0.05$).

II. Physical properties of CS-based SFSB films.

Analysis of physical properties of thin films

The thickness of the film is one of the important parameters for determining its physical properties [33]. As shown in **Table II**, with an increase in SFSB content, the thickness of the film also increases significantly. This is because the addition of SFSB increases the solids content in the film, disrupts the original organizational structure of the film matrix, and results in a thicker film [34].

Due to the interaction between chitosan and SFSB, the interaction between chitosan and water was limited, resulting in a decrease in the moisture content of the film with the addition of SFSB [4]. As can be seen from Table II, compared to the original swelling property of the CS film, the swelling degree of the CS film with SFSB added was significantly reduced, and the hydrophilic groups in the chitosan molecules are the main reason for the swelling behavior of the film [35]. Strong hydrogen bonds are formed between the substances in SFSB and the chitosan, thus reducing the swelling degree of the composite film. According to the results, the water solubility of the film gradually decreases with the increase of SFSB. This may be because the interaction between the chitosan chain and SFSB is enhanced, reducing the affinity of the chitosan chain to water, and thus reducing the water solubility of the CS film.

The hydrophobicity of the film surface was measured by contact angle. The results show that the addition of SFSB significantly increases the contact angle of the film, which may be due to the fact that the polyphenols and other compounds in SFSB are included in the chitosan network, and the COO^- group in SFSB can also interact with the $NH3^+$ group in chitosan, which reduces the availability of functional groups for the formation of hydrogen bond between CS and SFSB and water. The wettability of the film is reduced [36,37], so the addition of SFSB enhances the water resistance of the CS film.

Water vapor permeability is one of the important parameters in the design of food packaging materials. Low WVP can protect products and slow down the deterioration and decay of packaged food [38]. As seen in Table II, as the SFSB content gradually increases from 0% to 40%, the WVP decreases significantly from 0.456 to 0.364 g·mm/(m²·d·KP). This reduction is likely associated with the interaction between the amino group in CS and the carboxyl group and hydroxyl group in SFSB, which narrows the passage for water molecules [39]. The addition of SFSB increased the hydrophobicity and thickness of the film and decreased the water absorption of the film. In addition, the intermolecular hydrogen bond formed between SFSB and CS reduces the hydrophilic groups in the film, thus reducing the affinity of the film to water molecules [40].

Optical properties of films

The color of the film is shown in **Fig. 1a**. The CS film is almost colorless and transparent, while the color of CS-SFSB films deepens significantly with the increase of SFSB. As can be seen from **Table III**, L* value (brightness) decreases significantly, indicating that with the increase of SFSB, the film becomes darker, and the decrease of brightness of the film helps to prevent the oxidation and deterioration of food due to exposure to visible light [41,42]. The a* value (green to red) significantly decreased and b* value (blue to yellow) significantly increased, indicating that SFSB has a higher impact on the color of the film due to its inherent yellow color, making the film yellowing increase with the increase of its content. Rambabu [11] et al. also obtained similar results by adding mango leaf extract into CS film. The whiteness of the film significantly decreased and the opacity significantly increased, enabling it to preserve white-sensitive food materials [43].

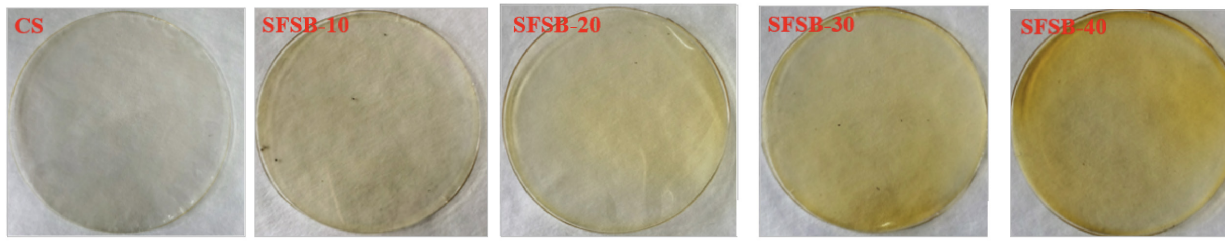

(a)

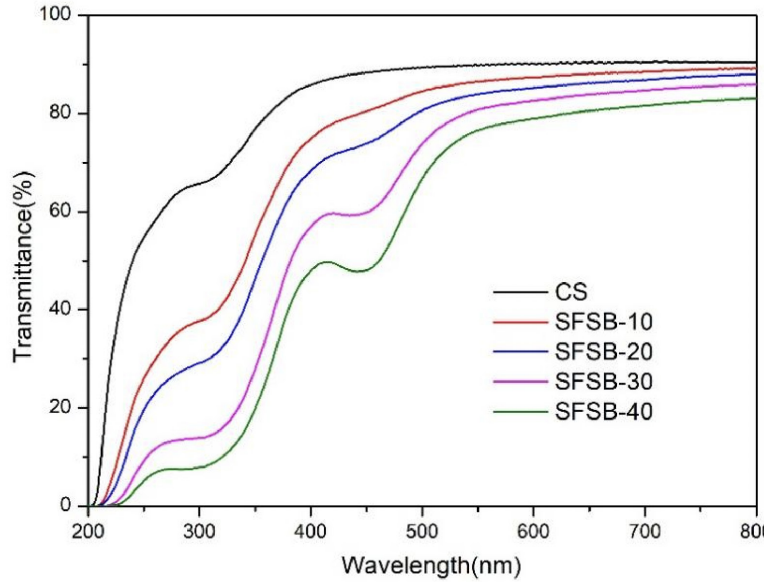

(b)

1. a) Color characteristics and b) transmittance of chitosan (CS) and chitosan-*Stachys floridana *Shuttlew. ex Benth (CS-SFSB) films.

Films	L*	a*	b*	Whiteness Index	Opacity
CS	68.94 ± 0.15^{a}	-1.77 ± 0.03^{a}	4.19 ± 0.07^{a}	36.17 ± 0.05^{a}	1.00 ± 0.08^{a}
SFSB-10	68.24 ± 0.11^{a}	-3.49 ± 0.10^{b}	10.81 ± 0.05^{b}	30.48 ± 0.06^{b}	1.50 ± 0.06^{c}
SFSB-20	67.79 ± 0.05^{b}	-4.41 ± 0.06^{d}	15.50 ± 0.05^{c}	26.84 ± 0.08^{b}	1.98 ± 0.10^{b}
SFSB-30	67.39±0.03^{c}	-5.80 ± 0.02^{c}	24.36 ± 0.10^{d}	22.18 ± 0.04^{a}	2.17 ± 0.11^{d}
SFSB-40	66.46±0.07^{d}	-5.89 ± 0.04^{c}	26.51± 0.11^{d}	19.24 ± 0.10^{d}	3.96 ± 0.09^{c}

CS: chitosan; SFSB: *Stachys floridana* Shuttlew. ex Benth; L*: luminosity; a*: chromacity (red-green); b*: chromacity (yellow-blue).
Values were expressed as mean ± standard deviation, and each experiment was repeated at least three times. Values with different superscript letters (a-d) indicated significant differences by Tukey's test ($p < 0.05$).

III. Color, whiteness, and opacity of films with different SFSB concentrations.

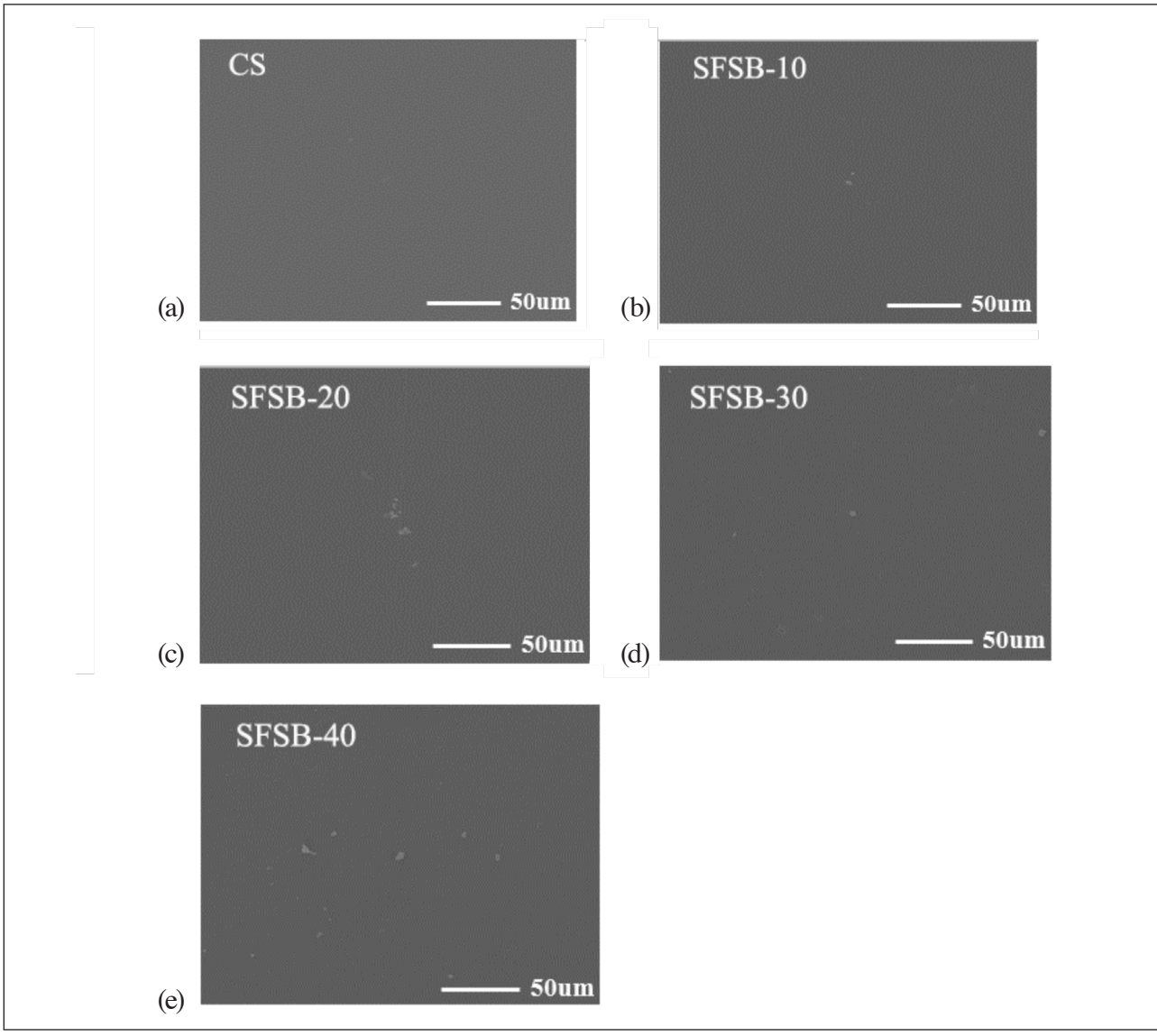

2. Scanning electron microscope (SEM) images of CS and CS-SFSB films.

Figure 1b shows the transmittance of the film. Compared with the film without SFSB, the CS film showed the highest transmittance. With the addition of SFSB, the transmittance of the film gradually decreased, indicating that the addition of extracts in the film matrix reduced the transparency of the film. This may be due to the fact that the substances in SFSB have strong absorption ability to UV, and the distribution of these substances in the film can scatter the light or block its propagation [44,45]. This helps to protect food from UV-induced oxidation and facilitates food storage.

SEM analysis

Figure 2 shows an SEM image of the prepared film. With the increase of SFSB, the roughness of the surface of the film gradually increased, but the surface was still smooth, with no bubbles, pores, or holes. This indicated that the extract was evenly distributed in the film without any obvious agglomeration, maintaining a smooth, uniform, and ordered structure of the film and good compatibility with CS. This may be due to the hydrophilicity of CS [7]. When SFSB extract is added to the film, due to the interactions between polyphenols, uronic acid, and CS in the extract, the film becomes thicker and denser, so the tight film structure reduces the WVTR of the film [46]. For example, the data obtained in the experiment remained consistent.

FTIR analysis

In order to explore the possible interaction between SFSB extract and chitosan, FTIR spectral analysis was performed. **Figure 3** shows the correlation spectra of each film. The results of FTIR spectroscopy show that the characteristic peaks of the films have slight changes. The peak value of the film near 3280 cm^{-1} was attributed to the tensile vibration of O-H and N-H of the CS film [47], but with the differ-

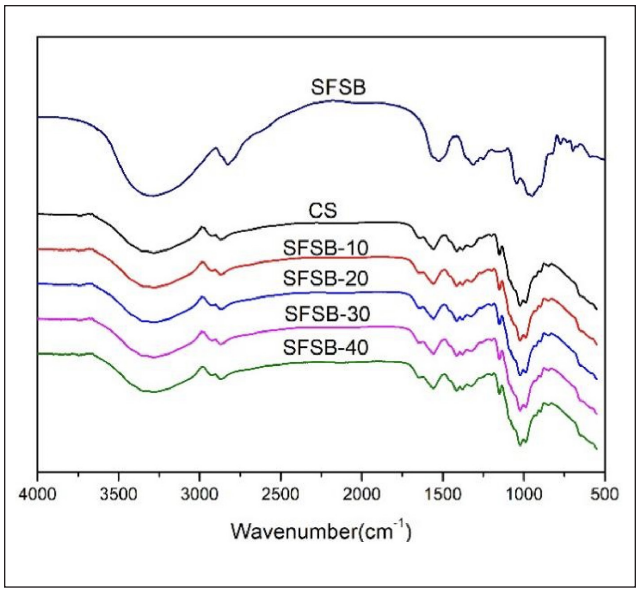

3. Fourier transform infrared (FTIR) spectra of SFSB and films.

ent amount of SFSB extract added, the peak value of the film shifted slightly and widened, which may be due to the corresponding groups in the CS bonded with the extract to form hydrogen bonds [48]. As can be seen from the Fig. 3, the addition of SFSB extract did not cause changes in the chemical structure of the CS film, indicating that the interaction between SFSB extract and the CS film was mainly physical [49]. Due to the hydrophilicity of chitosan, the SFSB and chitosan network have integrity [50]. Similarly, with the increase of SFSB concentration, the wave number of some peaks shifts. This indicates the interaction between CS film and SFSB, which may be caused by the reaction of -NH_2 in CS with phenol-OH and -COOH in SFSB [51]. Therefore, the main structure of the chitosan network remained unchanged when different concentrations of SFSB were added.

TGA results

The thermal stability of CS-SFSB films was tested by TGA. As shown in **Fig. 4**, the thermal decomposition of the film is mainly divided into three stages. The first stage (40°C–150°C) was mainly evaporation of water and volatile substances. The second stage (160°C–230°C) was associated with the degradation of glycerol and some low molecular weight components of the components [52]. The third stage (230°C–400°C) has been attributed to the depolymerization and pyrolysis of chitosan in the film [53]. The weight loss of the film in the first stage was lower than that of the CS film. This was consistent with the previous results that the water content of CS-SFSB films were lower than that of CS film. In general, the thermal stability of CS-SFSB films increases with the increase of SFSB, indicating that the addition of SFSB can improve the thermal stability of CS film. The TGA heat maps of the films showed a similar pattern, with no significant change in the thermal degradation pattern of the films. Therefore, the compatibility between SFSB and CS film was confirmed.

The DTG curve is plotted with temperature as the abscissa and the rate of mass change (dm/dT) as the ordinate. The DTG curve reflects the relationship between the rate of mass change and temperature, with smaller values on the ordinate indicating faster rates of mass loss. As shown in Fig. 4, the thermal decomposition rate of the films can be divided into three main stages. In the first stage (40°C–170°C), the thermal decomposition rate gradually increases, which is related to the evaporation of water and volatile substances, as well as the initial degradation of glycerol and film components [52]. In the second stage (170°C–270°C), the thermal decomposition rate fluctuates, which is associated with the degradation of different film components and the initial depolymerization and pyrolysis of chitosan. In the third stage (270–400°C), as the initial depolymerization

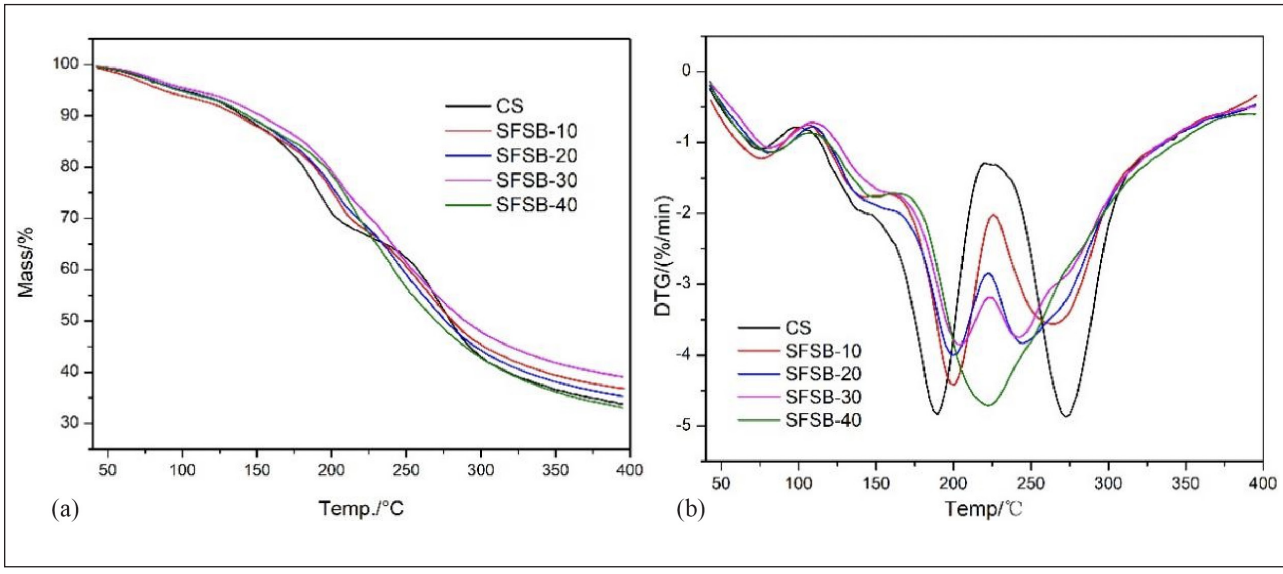

4. Thermogravimetric analysis (TGA) of CS and CS-SFSB films.

and pyrolysis of chitosan are completed, the subsequent reaction rate of thermal decomposition gradually decreases. In the first stage, the DTG curve of the CS-SFSB film is significantly higher than that of the CS film. In the second stage, the peak of the DTG curve of the CS-SFSB film is also more gradual compared to the peak of the DTG curve of the CS film, indicating that the addition of SFSB can enhance the thermal stability of the CS film. The similar trend in the shape of the curves also confirms the compatibility between SFSB and the CS film [53].

Mechanical strength

The stress-strain curves of CS and CS-SFSB films are shown in **Fig. 5**. The mechanical strength of the film mainly depends on the composition of the polymer and the intermolecular forces, as well as the microstructure of the film [54]. In the film stress, SFSB addition caused a significant difference. Specifically, when SFSB is from 0 to 40%, the stress of the film increases first and then decreases. The stress reaches the maximum value of 20.28 MPa at 10%, and decreases gradually with the increase of the addition amount, dropping to 10.04 MPa at 40%. This may be due to the fact that a small amount of SFSB interacts with CS to produce a strong interfacial binding force [55], but excessive addition of SFSB hinders the interaction between polymer chains, thus reducing the stress of CS film. Compared with pure CS film, the strain of thin film increases slightly, reaching the maximum 50.49% at 30%. This indicates that SFSB can be used as a reinforcing filler to strengthen the membrane network [40], which can increase the strain to some extent. However, when the addition amount is too large, it will lead to the discontinuity of the membrane structure and reduce the strain to some extent. This difference may also be related to the higher concentration of glycerol added in this experiment. The higher concentration of glycerol reduces the intermolecular attraction of chitosan chain and increases the mobility of polymer, thus increasing the strain of thin film [56].

Antioxidant and bacteriostatic properties

The DPPH and ABTS free radical scavenging experiments were used to investigate the antioxidant properties of the films. This study showed that the antioxidant activity was positively correlated with the concentration of SFSB extract in the film. With the increase of SFSB extract in the film, the scavenging rate of DPPH free radical was significantly increased. When the amount of SFSB extract was increased to 40%, the antioxidant activity of the film was increased by 181.8% compared with that of the film without SFSB extract. Chitosan film has slight oxidation resistance, which may be related to its free amino ($-NH_2$) groups and the formation of stable macromolecular free radicals.

The discoloration experiment of ABTS radical also showed the same trend. The higher the concentration of SFSB extract, the more complete ABTS free radical scavenging. When the addition amount is 40%, the clearance rate of the film reaches 70.89%, which is 224.64% higher than that of the film without addition. The clearance rate of pure CS film also reached 21.84 %, which was higher than that of the DPPH method, mainly because the ABTS method was more sensitive to the antioxidant activity of lipophilic compounds and easier to obtain higher antioxidant activity [58].

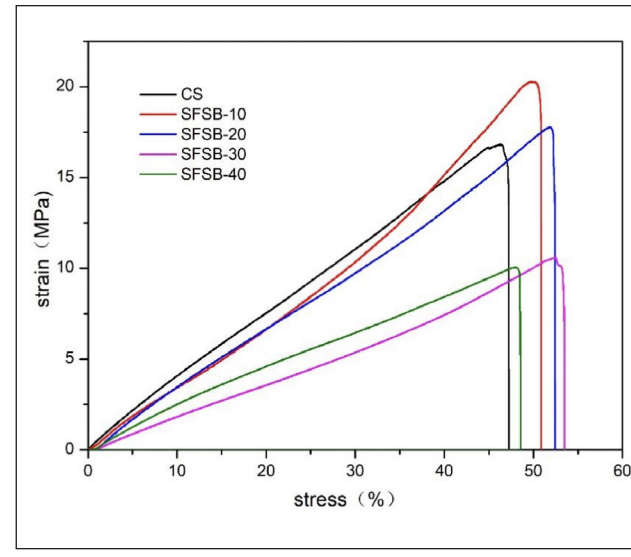

5. Stress-strain curves of CS and CS-SFSB films.

The bacteriostasis of the prepared films was evaluated using *Escherichia coli* and *Staphylococcus aureus*. As can be seen from the **Fig. 6c** and Fig. 6d, there is no obvious bacteriostatic zone in CS film, and CS-SFSB films have obvious inhibitory effect on the growth of *Escherichia coli* and *Staphylococcus aureus*; also, with the increase of SFSB extract concentration, the bacteriostatic zone increases. This may be due to the fact that SFSB extract acting on the bacterial cell film at a certain concentration changed its fluidity and permeability or the combination of specific sugar groups and proteins on its surface; destroyed the molecular structure of the bacterial cell film, causing the death of the bacteria; or concentrated on the surface of the bacteria, inhibiting its metabolism and causing its death [15].

Biodegradability

Figure 7 shows the visual images of CS film and SFSB film before and after biodegradation experiments. It can be seen from the figure that the soil biodegradation rate of CS film increases significantly after SFSB is added to the film. After 14 days, the film with SFSB added had broken significantly and was almost integrated into the soil. This may be because the protein in SFSB provides the nitrogen source for microorganisms, and other components provide the carbon source for microorganisms. In the humid environment, the activity of microorganisms in the soil is improved, thus the degradation rate of the film in the soil is increased [59]. Adding SFSB to CS film improves its biodegradability with

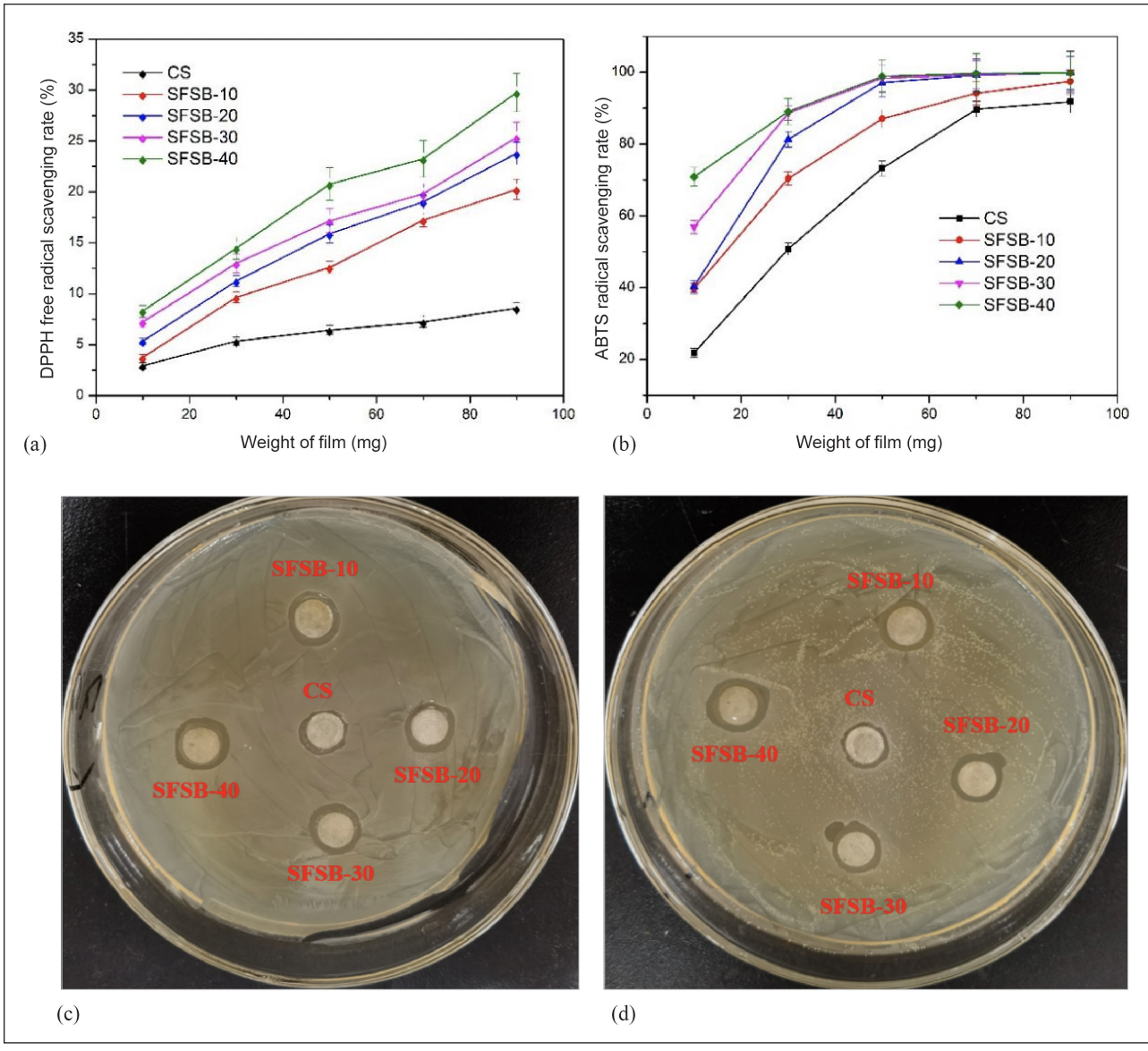

***6. a) DPPH free radical scavenging rate of CS and CS-SFSB films; b) ABTS scavenging rate; c) bacteriostasis of* Escherichia coli*; and d) bacteriostasis of* Staphylococcus aureus.**

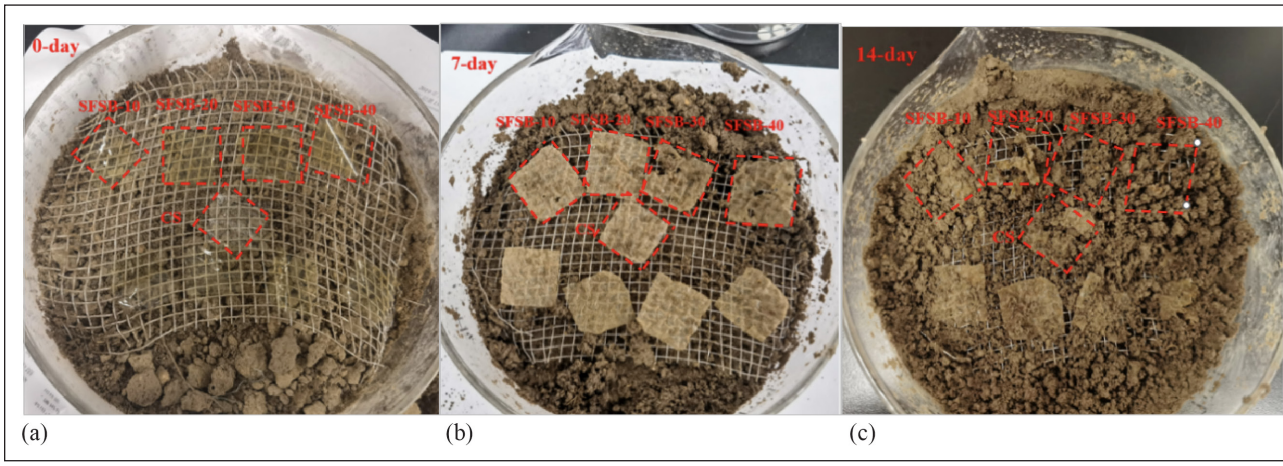

7. Chitosan film and CS-SFSB film before and after biodegradation experiment.

faster degradation speed and smaller burden on the environment. This was similar to the results obtained by Riaz et al. [8], where chives root extract was added to CS film, and it was consistent with the results obtained by Yilmaz et al., where leaf extract was added to CS film [35].

CONCLUSION

In this study, the discussion centered on the effects of different contents of extract and chitosan on the preparation of composite films. The key findings revealed remarkable improvements in the physicochemical properties of CS films upon the addition of various amounts of *Stachys floridana* Shuttlew. ex Benth (SFSB) extract. Specifically, the thickness, water content, water solubility, expansibility, transparency, and water vapor permeability of the CS films were notably reduced. Additionally, the contact angle of the films increased significantly, from 75.6° to 89.3°. Furthermore, the mechanical properties, UV barrier function, and thermal stability of the films were substantially enhanced. Notably, the CS-SFSB films exhibited pronounced antioxidant and bacteriostatic properties, along with improved biodegradability.

These enhancements can be attributed to the interaction between the SFSB extract and chitosan matrix. The extract components likely reinforced the film structure, reducing water absorption and permeability, thereby increasing the contact angle and improving barrier properties. Additionally, the bioactive compounds in the SFSB extract contributed to the enhanced mechanical strength, UV resistance, and thermal stability of the films. The antioxidant and antibacterial properties of the extract further augmented the functionality of the CS-SFSB films, making them suitable for food packaging applications. Lastly, the improved biodegradability underscores the environmental friendliness of these composite films, suggesting a promising future for their development as sustainable packaging materials. **TJ**

LITERATURE CITED

1. Andrade, R.M.S., Ferreira, M.S.L., and Gonçalves, É.C.B.A., *J. Food Sci.* 81(2): E412(2016). https://doi.org/10.1111/1750-3841.13192.
2. Valencia-Chamorro, S.A., Palou, L., Del Río, M.A., et al., *Crit. Rev. Food Sci. Nutri.* 51(9): 872(2011). http://dx.doi.org/10.1080/10408398.2010.485705.
3. Otoni, C.G., Avena-Bustillos, R.J., Azeredo, H.M.C., et al., *Compr. Rev. Food Sci. Food Saf.* 16(5): 1151(2017). https://doi.org/10.1111/1541-4337.12281.
4. Zhang, X., Lian, H., Shi, J., et al., *Int. J. Biol. Macromol.* 148: 1242(2020). https://doi.org/10.1016/j.ijbiomac.2019.11.108.
5. Dash, M., Chiellini, F., Ottenbrite, R.M., et al., *Prog. Polym. Sci.* 36(8): 981(2011). https://doi.org/10.1016/j.progpolymsci.2011.02.001.
6. Ferreira, A.S., Nunes, C., Castro, A., et al., *Carbohydr. Polym.* 113: 490(2014). https://doi.org/10.1016/j.carbpol.2014.07.032.
7. Kadam, A.A., Singh, S., and Gaikwad, K.K., *Food Control* 124: 107877(2021). https://doi.org/10.1016/j.foodcont.2021.107877.
8. Riaz, A., Lagnika, C., Luo, H., et al., *Int. J. Biol. Macromol.* 150: 595(2020). https://doi.org/10.1016/j.ijbiomac.2020.02.078.
9. Siripatrawan, U. and Harte, B.R., *Food Hydrocolloids* 24(8): 770(2010). https://doi.org/10.1016/j.foodhyd.2010.04.003.
10. Vieira, J.M., Flores-López, M.L., de Rodríguez, D.J., *Postharvest Biol. Technol.* 116: 88(2016). https://doi.org/10.1016/j.postharvbio.2016.01.011.
11. Rambabu, K., Bharath, G., Banat, F., et al., *Int. J. Biol. Macromol.* 126: 1234(2019). https://doi.org/10.1016/j.ijbiomac.2018.12.196.
12. Ma, L.P., Qin, C.L., Qiu, Z.J., et al., *Sci. Techol Food Ind.* 34(9): 356(2013).
13. Ma, L.P., Zhao, J.F., Wang, L., et al., *Food Sci. Technol.* 38(5): 217(2013).
14. Li, X.Y., Qi, P.B., Gong, Q.H., et al., *J. Bengbu Med. Coll.* 37(3): 254(2012).
15. Zhang, X.W., Wang, S.M., Wang, D.G., et al., *Food Res. Dev. (Tianjin, China)* 32(7): 25(2011).
16. Ma, L., Gan, D., Wang, M., et al., *Carbohydr. Polym.* 87(2): 1390(2012). https://doi.org/10.1016/j.carbpol.2011.09.032.
17. Xianfeng, Z., Guidong, H., Yan, C., et al., *J. Food Sci. Technol.* 50(5): 942(2013). https://doi.org/10.1007/s13197-011-0413-1.
18. Ma, L., Qin, C., Wang, M., et al., *Food Chem. Toxicol.* 60: 269(2013). https://doi.org/10.1016/j.fct.2013.07.060.
19. Lin, J., Li, X., Han, L., et al., *Bot. Stud.* 55(1): 16(2014). https://doi.org/10.1186/1999-3110-55-16.
20. Li, X., Hu, Q., Jiang, S., et al., *J. Saudi Chem. Soc.* 19(4): 454(2015). https://doi.org/10.1016/j.jscs.2014.06.004.
21. Bradford, M.M., *Anal. Biochem.* 72(1): 248(1976). https://doi.org/10.1006/abio.1976.9999.
22. Chen, S., Zhang, Z., Wei, X., et al., *Food Biosci.* 49: 101893(2022). https://doi.org/10.1016/j.fbio.2022.101893.
23. Jiang, L., Luo, Z., Liu, H., et al., *Foods* 10(11): 2834(2021). https://doi.org/10.3390/foods10112834.
24. Riaz, A., Lagnika, C., Luo, H., et al., *Int. J. Biol. Macromol.* 150: 595(2020). https://doi.org/10.1016/j.ijbiomac.2020.02.078.
25. Stalder, A.F., Kulik, G., Sage, D., et al., *Colloids Surf., A* 286(1): 92(2006). https://doi.org/10.1016/j.colsurfa.2006.03.008.
26. Bi, F., Zhang, X., Bai, R., et al., *Int. J. Biol. Macromol.* 134: 11(2019). https://doi.org/10.1016/j.ijbiomac.2019.05.042.
27. Silva, I.D.D.L., Moraes Filho, L.E.P.T., Caetano, V.F., et al., *LWT* 144: 111215(2021). https://doi.org/10.1016/j.lwt.2021.111215.
28. Li, X., Ouyang, X., Cai, R. et al., 24(11): 2039(2019). https://doi.org/10.3390/molecules24112039.
29. Genskowsky, E., Puente, L.A., Pérez-álvarez, J.A., et al., *LWT – Food Sci. Technol.* 64(2): 1057(2015). https://doi.org/10.1016/j.lwt.2015.07.026.
30. Sun, L., Sun, J., Chen, L., et al., *Carbohydr. Polym.* 163: 81(2017). https://doi.org/10.1016/j.carbpol.2017.01.016.
31. Medina Jaramillo, C., Gutiérrez, T.J., Goyanes, S., et al., *Carbohydr. Polym.* 151: 150(2016). https://doi.org/10.1016/j.carbpol.2016.05.025.
32. Piñeros-Hernandez, D., Medina-Jaramillo, C., López-Córdoba, A., et al., *Food Hydrocolloids* 63: 488(2017). https://doi.org/10.1016/j.foodhyd.2016.09.034
33. Delgado, J.F., Peltzer, M.A., Wagner, J.R., et al., *Eur. Polym. J.* 99: 9(2018). https://doi.org/10.1016/j.eurpolymj.2017.11.051.

34. Sivarooban, T., Hettiarachchy, N.S., and Johnson, M.G., *Food Res. Int.* 41(8): 781(2008). https://doi.org/10.1016/j.foodres.2008.04.007.

35. Yilmaz, P., Demirhan, E., and Ozbek, B., *Food Biosci.* 46: 101542(2022). https://doi.org/10.1016/j.fbio.2021.101542.

36. Ojagh, S.M., Rezaei, M., Razavi, S.H., et al., *Food Chem.* 120(1): 193(2010). https://doi.org/10.1016/j.foodchem.2009.10.006.

37. Jindal, M., Kumar, V., Rana, V., et al., *Int. J. Biol. Macromol.* 52: 77(2013). https://doi.org/10.1016/j.ijbiomac.2012.10.020.

38. Wu, J., Sun, X., Guo, X., et al., *Food Bioprocess Technol.* 11(2): 447(2018). https://doi.org/10.1007/s11947-017-2021-1.

39. Zhang, W., Li, X., and Jiang, W., *Int. J. Biol. Macromol.* 154: 1205(2020). https://doi.org/10.1016/j.ijbiomac.2019.10.275.

40. Jiang, L., Jia, F., Han, Y., et al., *Carbohydr. Polym.* 261: 117877(2021). https://doi.org/10.1016/j.carbpol.2021.117877.

41. Hanani, Z.A.N., Yee, F.C., and Nor-Khaizura, M.A.R., *Food Hydrocolloids* 89: 253(2019). https://doi.org/10.1016/j.foodhyd.2018.10.007.

42. Riaz, A., Lei, S., Akhtar, H.M.S., et al., *Int. J. Biol. Macromol.* 114: 547(2018). https://doi.org/10.1016/j.ijbiomac.2018.03.126.

43. Yang, H., Li, J.G., Wu, N.F., et al., *Food Hydrocolloids* 50: 211(2015). https://doi.org/10.1016/j.foodhyd.2015.03.028.

ABOUT THIS PAPER

Cite this article as:
Zhao, Q., Liu, S., Li, J., et al., *TAPPI J.* 24(6): 301(2025). https://doi.org/10.32964/TJ24.6.301

DOI: https://doi.org/10.32964/TJ24.6.301

ISSN: 0734-1415

Publisher: TAPPI Press

About this journal

44. Hopkins, E.J., Chang, C., Lam, R.S.H., et al., *Food Res. Int.* 67: 418(2015). https://doi.org/10.1016/j.foodres.2014.11.040.

45. Jiang, L., Luo, Z., Liu, H., et al., *Foods* 10(11): 2834(2021). https://doi.org/10.3390/foods10112834.

46. Atarés, L., Pérez-Masiá, R., and Chiralt, A., *J. Food Eng.* 104(4): 649(2011). https://doi.org/10.1016/j.jfoodeng.2011.02.005.

ABOUT THE AUTHORS

We chose this topic for research because it addresses the growing need for ecofriendly and biodegradable packaging materials to mitigate environmental pollution. This research complements previous research by exploring a novel plant extract, *Stachys floridana* Shuttlew. ex Benth (SFSB), to enhance chitosan film properties, providing new insights.

The most difficult aspect of this study was ensuring uniform extract distribution. This was addressed by optimizing the mixing and using ultrasonic degassing.

Through our study, we found that SFSB extract significantly improved chitosan film's antioxidant, antibacterial, and biodegradability properties. It was particularly interesting to observe the rapid increase in chitosan film biodegradability upon SFSB extract addition.

Food packaging producers can benefit from the information here by considering how incorporation of SFSB extract into chitosan packaging contributes to ecofriendly and functional products. Our next steps are larger-scale experiments to validate findings and explore commercial viability for industrial use.

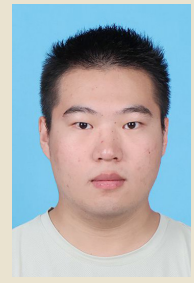

Zhao

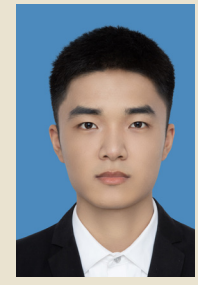

Shun Liu

J. Li

H. Liu

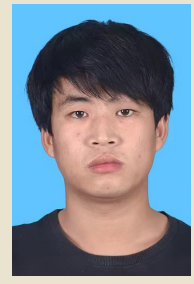

Sheng Liu

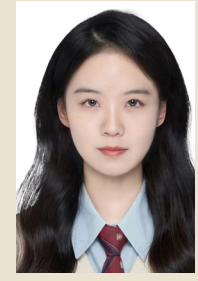

Q. Wang

Y. Li

H. Wang

Zhao, Shun Liu*, Sheng Liu, Q. Wang, Y. Li, and H. Wang are Master's candidates; J. Li* holds a Master's degree; and H. Liu is associate professor in the College of Light Industry Science and Engineering, Tianjin Key Laboratory of Pulp & Paper, at Tianjin University of Science and Technology in Tianjin, P.R. China. Email Liu at liuhaitang@tust.edu.cn.*

**Co-authors Zhao, Shun Lieu, and J. Li contributed equally to this work and are considered first authors.*

47. Su, L., Huang, J., Li, H., et al., *Int. J. Biol. Macromol.* 172: 231(2021). https://doi.org/10.1016/j.ijbiomac.2021.01.056.
48. Bi, F., Zhang, X., Bai, R., et al., *Int. J. Biol. Macromol.* 134: 11(2019). https://doi.org/10.1016/j.ijbiomac.2019.05.042.
49. Li, Z., Yang, Y., Liu, M., et al. *Biomed. Pharmacother.* 137: 111393(2021). https://doi.org/10.1016/j.biopha.2021.111393.
50. Meng, W., Shi, J., Zhang, X., et al., *Int. J. Biol. Macromol.* 152: 137(2020). https://doi.org/10.1016/j.ijbiomac.2020.02.235.
51. Medina Jaramillo, C., Gutiérrez, T.J., Goyanes, S., et al., *Carbohydr. Polym.* 151: 150(2016). https://doi.org/10.1016/j.carbpol.2016.05.025.
52. Ramziia, S., Ma, H., Yao, Y., et al., *J. Appl. Polym. Sci.* 135(10): 45781(2018). https://doi.org/10.1002/app.45781.
53. Pastor, C., Sánchez-González, L., Chiralt, A., et al., *Food Hydrocolloids* 30(1): 272(2013). https://doi.org/10.1016/j.foodhyd.2012.05.026.
54. Park, S. and Zhao, Y., *J. Food Sci.* 71(2): E95(2006). https://doi.org/10.1111/j.1365-2621.2006.tb08902.x
55. Bourbon, A.I., Pinheiro, A.C., Cerqueira, M.A., et al., *J. Food Eng.* 106(2): 111(2011). https://doi.org/10.1016/j.jfoodeng.2011.03.024.
56. Yen, M., Yang, J., and Mau, J., *Carbohydr. Polym.* 74(4): 840(2008). https://doi.org/10.1016/j.carbpol.2008.05.003.
57. Alam, M.N., Bristi, N.J., and Rafiquzzaman, M., *Saudi Pharm. J.* 21(2): 143(2013). https://doi.org/10.1016/j.jsps.2012.05.002.
58. Gasti, T., Dixit, S., Sataraddi, S.P., et al., *J. Polym. Environ.* 28(11): 2918(2020). https://doi.org/10.1007/s10924-020-01832-6.